PHYSICAL REVIEW B VOLUME 23, NUMBER 2 15 JANUARY 1981

Recombination in *a*-Si:H: Auger effects and nongeminate recombination

R. A. Street
Xerox Palo Alto Research Center, Palo Alto, California 94304
(Received 30 May 1980)

Excitation-intensity effects in the luminescence of plasma-deposited *a*-Si:H are described. At low temperatures (< 50 K) the luminescence quantum efficiency decreases at high excitation levels, and the results are interpreted as indicating Auger recombination of neighboring geminate electron-hole pairs. At high temperatures (> 50 K) the quantum efficiency increases with excitation intensity, particularly in samples of low spin density. This result is attributed to the onset of bimolecular, nongeminate, radiative recombination. Analysis of the rate equations shows that the primary nonradiative process in *a*-Si:H involves capture of free carriers at singly occupied dangling-bond defects. Estimates of the recombination rates are obtained.

I. INTRODUCTION

The low-temperature luminescence of undoped *a*-Si:H is dominated by a broad transition with its peak at 1.3–1.4 eV which is attributed to recombination of electrons and holes at the band edges.[1–6] Studies of the time decay of luminescence have been very informative in determining the details of the recombination kinetics.[7] A model has been developed in which the recombination is by radiative tunneling of carriers in localized band-tail states. Recombination is geminate at low excitation intensities, becoming nongeminate when the electron-hole pair density exceeds about 2×10^{18} cm^{-3}. This change of mechanism is attributed to the overlap of adjacent pairs. At elevated temperatures, the average decay time decreases and an asymptotic $t^{-3/2}$ decay of the luminescence intensity is observed.[8] This result is attributed to the thermally activated diffusion apart of the electron-hole pair. Accompanying this separation is a temperature-dependent quenching of the luminescence intensity. The activation energy for this process ranges between 0.07 and 0.23 eV in different measurements,[1,4,6,7] but the universal interpretation is that the activated process is the ionization of the electron-hole pair. This interpretation of the luminescence implies that ionized carriers recombine nonradiatively. In this paper we report on the temperature dependence and excitation-intensity dependence of the luminescence, and show that the nonradiative recombination occurs predominately by capture at dangling-bond defects. However if the dangling-bond density is sufficiently low the free carriers can recombine radiatively by a nongeminate process.

The presence of dangling bonds is also known to reduce the low-temperature quantum efficiency.[9] The explanation given is that electrons tunnel from the band tail into a nearby defect. We show that the temperature dependence of the lunimescence is altered by the dangling bonds, and that the changes are in agreement with the tunneling model.

The temperature dependence of luminescence betweeen 0 and 50 K has been a puzzling feature in the past. Some studies find the unusual property of an increase in quantum efficiency with temperature,[3,6,7] while other data find this effect to be absent.[1,4] The effect is accompanied by a decrease in the mean radiative decay time, attributed, in this temperature range, to the diffusion of the electron-hole pair towards each other.[7] However the change of luminescence intensity requires a competing nonradiative mechanism, the origin of which was unknown. The experiments described here show that this nonradiative process disappears at low excitation intensities, and therefore we attribute the effect to the Auger recombination of neighboring geminate pairs.

II. EXPERIMENTAL RESULTS

The method of preparing *a*-Si:H, and the techniques used for measuring luminescence have been described elsewhere.[7,9] Suitable choice of deposition conditions results in samples with a spin density varying from 3×10^{15} cm^{-3} to above 10^{18} cm^{-3}. At low temperature and low excitation intensity, a substantial fraction of the total luminescence decay occurs at time constants larger than 1 msec. Therefore to avoid any possibility of signal roll-off due to modulation of the excitation light at too high frequency, all the data reported here use unmodulated excitation, and an $S-1$ photomultiplier in the photon-counting mode for detection. Roll-off effects may have contri-

buted to the magnitude of the low-temperature change in intensity reported previously.[7] The photomultiplier also provided the large signal-to-noise ratio required in measurements of the intensity dependence. The discussion of the data is divided into the low-temperature (0–50 K) and high-temperature (> 50 K) regions. As is more apparent from the discussion, this distinction corresponds to whether or not thermally activated ionization of the electron-hole pair occurs.

A. Low temperature (< 50 K)

Figure 1 shows examples of the temperature dependence of the luminescence intensity for various excitation intensities. This sample has the lowest measured dangling-bond density of any of our samples (spin density $\sim 3 \times 10^{15}$ cm^{-3}) and a high luminescence efficiency. The measurements are made near the peak of the luminescence spectrum. There is a small shift of the peak energy with temperature.[7] However the shift is independent of the excitation intensity, so that the data in Fig. 1 are directly comparable. It is found that the increase of luminescence intensity I_L is largest at the highest excitation power, but is virtually absent at low power. The absorption depth at 1.915 eV is about an order of magnitude larger than at 2.41 eV, and the change in I_L is smaller. In the limit of low excitation intensity, we observe an increase in I_L with temperature of about 2%. This change can be accounted for, within experimental uncertainty, by the temperature-dependent shift in energy of the luminescence spectrum, which changes the intensity at the wavelength of the measurement. Thus we conclude that the increase in I_L is completely absent at the lowest excitation intensity.

Figure 2 shows the relative temperature dependence of the ratio of I_L measured at high power (1 mW) and low power (0.01 mW) for the sample of Fig. 1, and for another sample with a spin density of 3×10^{17} cm^{-3} which has a low-temperature luminescence efficiency reduced by about an order of magnitude. The lower efficiency sample has a smaller change in I_L by about a factor of 5. It is not clear to what extent these results can account for the differing observations of others. For example Austin *et al.*[4] report no low-temperature change of I_L despite using samples of low defect density. However their excitation source is a xenon lamp and monochromator, and therefore it seems likely that the excitation

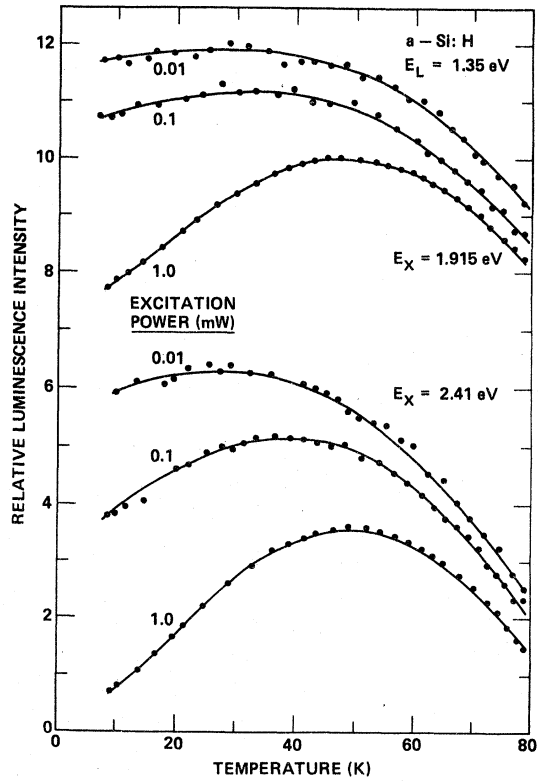

FIG. 1. Temperature dependence of the luminescence intensity in the range 0–80 K for various incident excitation powers and wavelengths as shown. The data are normalized such that the maximum intensity is 10 units of the vertical scale, and the different curves have offset zeros. The illumination spot diameter is 2 mm.

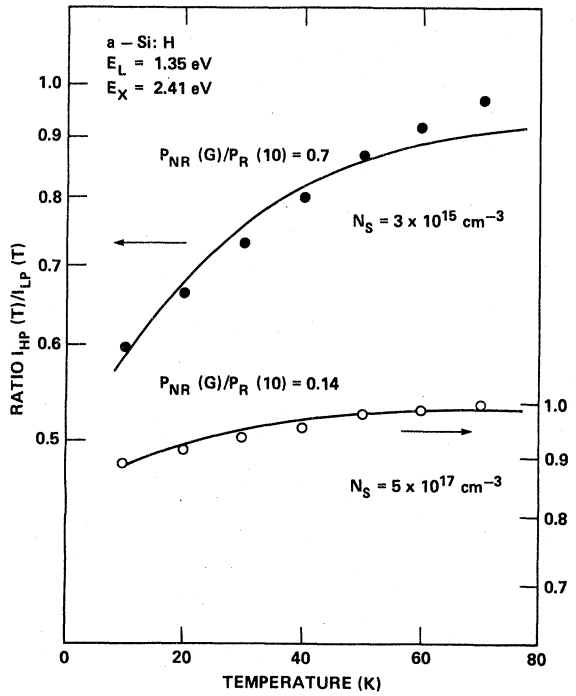

FIG. 2. Ratio of the luminescence efficiency measured at high excitation power I_{HP} (1 mW), to that at low power I_{LP} (0.01 mW), at different temperatures, for two samples of different ESR spin densities. The solid curves are fits to the data based on Eq. (1).

intensity is sufficiently low that the change in I_L is negligible. On the other hand, Collins *et al.*[10] find that in sputtered samples the change in I_L is not closely correlated with the luminescence intensity. Possibly the variation in the band gap with hydrogen partial pressure may be responsible because of the change in excitation density.

B. High temperatures (> 50 K)

We next describe results at temperatures above 50 K when ionization of electron-hole pairs is important. Figure 3 shows the temperature dependence of the luminescence intensity between 70 and 250 K for two different excitation powers (1 and 0.01 mW), and samples of differing spin density. The data are normalized to the maximum quantum efficiency of the brightest sample. The data are again measured near the peak of the low-temperature spectrum, and are not corrected for the temperature shift of the peak. The shift is substantial at high temperature[7] and introduces quite large errors in the absolute intensity. However to a good approximation the shift of the peak is independent of excitation intensity and sample, so that the various sets of data can again be directly compared. For the purpose of this paper we are only interested in relative changes, not in the absolute magnitudes. Two effects can be seen in Fig. 3. As the spin density of the sample increases, the low-temperature efficiency decreases, as was known from previous data.[9] However the thermal quenching is also reduced, so that about 200 K, the intensities of the different samples converge. Evidently the presence of dangling bonds changes the temperature dependence. The second effect is that the form of the temperature dependence is intensity dependent. This effect is particularly strong in the low spin-density sample. Above ~150 K the quantum efficiency is nearly an order of magnitude larger when the higher excitation intensity is used. As the spin density increases the effect of excitation intensity decreases. Note that this effect is different from the low-temperature behavior, in that it is larger and of the opposite sign. At about 50 K the efficiency is virtually independent of intensity, over the range investigated.

The intensity dependence of the quantum efficiency, and its dependence on spin density are seen in more detail in Fig. 4. This shows examples of the change of luminescence efficiency at 170 K with incident excitation intensity G, for different samples. The relative quantum efficiency $Y_L = I_L/G$ is plotted versus the excitation intensity G. In general Y_L is constant at the lowest values of G, above which it increases, and eventually goes through a maximum. At the highest excitation intensities there is some sample heating, which reduces I_L because of the strong temperature dependence at 170 K. This effect

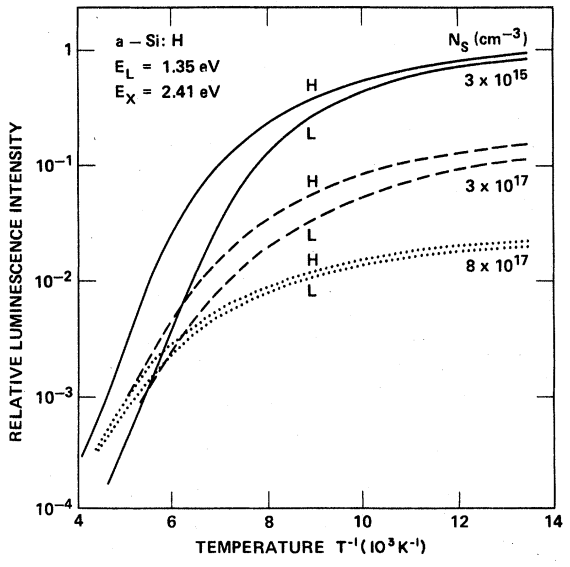

FIG. 3. Temperature dependence of the luminescence intensity measured at low (0.01 mW) and high (1 mW) excitation power for samples of different ESR spin density. The illumination spot diameter is 2 mm.

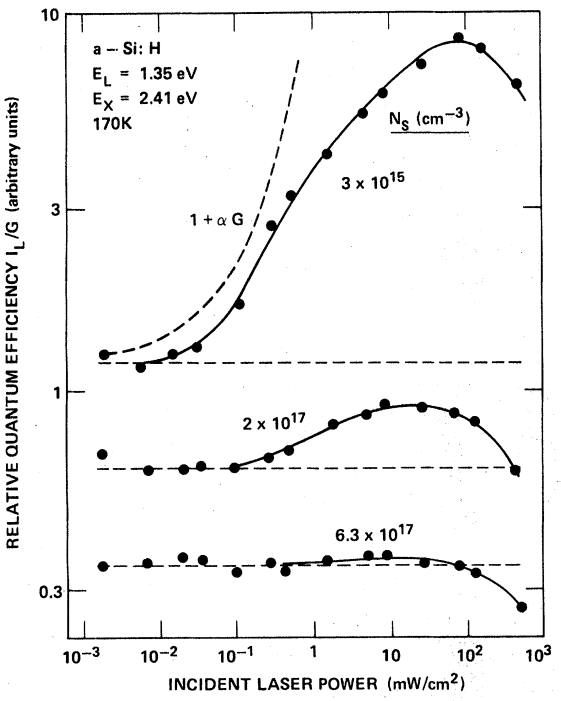

FIG. 4. Plot of the relative luminescence quantum efficiency vs incident excitation power for samples of differing spin density. Dashed curve illustrates the relation predicted by Eq. (10).

is minimized by measuring the luminescence in the first 100 msec of illumination. By comparing the calculated total temperature rise expected from the thermal properties of the sample substrate, with the observed decrease of luminescence intensity with time after illumination, we estimate that at the highest intensity, Y_L is underestimated by no more than $\sim 20\%$. Thus the flattening off of Y_L at high G in Fig. 4 is apparently a real effect, although the decrease above 10^2 mW/cm^2 may be an artifact due to the temperature rise.

Figure 4 confirms that the relative increase of Y_L is largest in samples with the smallest spin density N_S, and that the effect decreases steadily as N_S increases. We can define the enhancement of the quantum efficiency as $Y_{max}/Y_0 - 1$ where Y_{max} and Y_0 are the efficiencies at the peak and at the low intensity limit. We find that this parmater varies by about three orders of magnitude for undoped samples with spin densities ranging from 3×10^{15} up to 6×10^{17} cm^{-3}.

III. DISCUSSION

There are three specific features of the data which are discussed separately. These are the low-temperature (0–50 K) increase in I_L which depends on excitation intensity; the effect of spin density on the temperature dependence at low excitation intensity; and the intensity dependence and spin-density dependence of Y_L in the high-temperature region.

A. Low-temperature properties

Figure 1 shows that at sufficiently low excitation intensity, I_L is constant up to 30–40 K, above which I_L decreases. At high intensity I_L increases by up to 30%, reaching a peak at about 50 K. The measurements at different excitation wavelengths (giving different absorption depths) indicate that the excitation density rather than incident power is the important variable. Note however that the excitation density decreases exponentially into the sample, so that all the effects observed correspond to the appropriate average. A qualitative interpretation of the data is obtained by assuming that there is an intensity-dependent nonradiative process with rate $P_{NR}(G)$. Thus the luminescence efficiency is given by

$$Y_L = P_R/[P_R + P_{NR}(G) + P_{NR}(T)] \ , \qquad (1)$$

where P_R is the radiative rate, and $P_{NR}(T)$ is the temperature-dependent nonradiative rate attributed to ionization of the electron-hole pair. The real experimental situation corresponds to an appropriate site average of Eq. (1) for the distribution in the various rates. From the measurements at low G, it is evident that $P_{NR}(T)$ is negligible below 50 K, and so will be ignored in this discussion. It is known that P_R increases with temperature for reasons discussed elsewhere.[7,8] Thus Y_L will generally be temperature dependent even if $P_{NR}(T)$ is negligible. Of course if $P_{NR}(G)$ is also negligible, Y_L is constant (equal to unity) and this corresponds to the low intensity limit. When $P_{NR}(G)$ is comparable with P_R, the temperature-dependent increase in P_R causes Y_L to increase with temperature, as observed. In Fig. 2 the data are fitted to Eq. (1) using measured average values of P_R (Ref. 11) and a value of $P_{NR}(G)/P_R(0)$ which is independent of temperature, where $P_R(0)$ is the low-temperature value of P_R. Evidently Eq. (1) gives a reasonable description of the data. The deviation at high temperature for the low spin-density sample is caused by the high-temperature mechanism discussed in Sec. III C. The dependence on spin density can be understood in the following way. According to previous models[9,12] the dangling bonds act as a rapid sink for electron-hole pairs excited within about 100 Å of the defect. Their effect is therefore to reduce the population of electron-hole pairs. Thus the radiative component of the decay is equivalent to that occurring in a sample of low spin density and lower excitation intensity. From this discussion we conclude that the low-temperature behavior is determined by a nonradiative process whose rate increases with the density of optically excited electron-hole pairs.

We believe that this process is Auger recombination. We rule out reabsorption which is the only other possible mechanism that we are aware of. For the absorption depth of ~ 1000 Å, an unreasonably large induced absorption coefficient of $\sim 10^5$ cm^{-1} at the luminescence energy would be required. The Auger process has already been suggested by Rehm and Fischer[13] to account for a bimolecular nonradiative recombination process which they observe in time-solved measurements at high intensites. Since Auger recombination requires an additional carrier, the process is expected to be significant only when the geminate photogenerated electron-hole pairs overlap. Previous measurements[7] show that this occurs above an incident intensity of ~ 3 mW/cm^2, for excitation at 2.4 eV, which corresponds to a laser power of ~ 0.1 mW. (The unfocused laser spot has a diameter of ~ 2 mm.) The onset of the effect in Fig. 1 at about this intensity therefore supports the Auger model.

Figure 5 shows a schematic diagram of the Auger process. There are several different possible processes involving the two neighboring pairs, of which only two are shown. Various Auger processes are known to occur in semiconductors, with transition rates that are large enough to dominate over radiative recombination. One example involving three localized carriers is the neutral donor- or acceptor-bound exciton. The Auger process for this complex was first identified in GaP.[14] The Auger transition

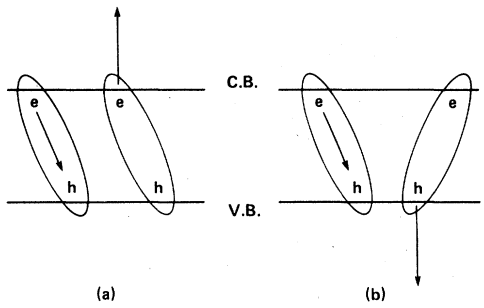

FIG. 5. Schematic illustration of two posssible nonradiative Auger recombination processes for two neighboring electron-hole pairs. Ovals are intended to denote geminate pairs.

rate of 10^7–10^8 sec^{-1} is about a factor 10^3 larger than the radiative rate. In the present situation the Auger rate will be much reduced by an overlap factor because the three particles are localized at different sites. Nevertheless, since rates of only $\sim 10^3$ sec^{-1} are required to explain the data, the mechanism is clearly plausible. Although there have been many calculations of the Auger rate for different physical situations,[15] none applies well to the present case. As an illustration, the Auger rate of the exciton bound to a neutral acceptor varies as approximately the 5th power of the acceptor binding energy.[16] This relation comes from the momentum-conservation requirement so that the rate depends on the portion of the Brillouin zone which contributes to the effective mass acceptor wave function. In an amorphous semiconductor the momentum-conservation requirement is generally assumed to be relaxed. This presumably weakens the dependence on binding energy and may result in a relative enhancement of the Auger rates. A detailed calculation for an amorphous semiconductor would be very valuable.

Further analysis of the recombination does not seem justified at this stage because of the lack of knowledge of the Auger rate. The problem is also complicated by the random distribution both of photoexcited pairs, and of the electron-hole separation within a pair, and by the possibility of nongeminate radiative transitions. We believe that the bimolecular recombination studied previously by Tsang and Street[7] is largely radiative as they assumed. If the Auger process were the only bimolecular mechanism, then the quantum efficiency should decrease more than the 30% observed in the data of Fig. 1. One simple argument can be made concerning this point. We assume that the electron Bohr radius is larger than that of the hole, and that wave function overlap is the determining factor in which type of transition dominates. Then one might expect that a four-particle configuration (two neighboring pairs) in which the electron-electron separation is less than the smallest electron-hole separation would favor Auger recombination, and if the reverse is true, radiative recombination would dominate. This argument predicts a maximum Auger contribution of $\sim 50\%$, which is consistent with the observations.

B. Temperature dependence in the low intensity limit

At sufficiently low excitation intensities, recombination is expected to be geminate. The lowest intensities used for the data of Fig. 4 correspond to an estimated photoexcited pair density of 10^{14}–10^{15} cm^{-3} at ~ 50 K, decreasing rapidly at higher temperature. The mean separation of pairs is therefore ~ 1000 Å or greater and a geminate process is certainly indicated. This section is concerned with the effect of dangling bonds with spin density N_S on the temperature dependence. As shown elsewhere,[9] the low-temperature quantum efficiency decreases when N_S is greater than $\sim 10^{17}$ cm^{-3}. A nonradiative process was proposed in which the electron tunneled to the dangling bond. For a random distribution of defects, the low-temperature quantum efficiency Y_L is given by[12]

$$Y_L = \exp(-\tfrac{4}{3}\pi R_c^3 N_S) \ , \tag{2}$$

with

$$R_c = \tfrac{1}{2} R_0 \ln(\omega_0/P_R) \ , \tag{3}$$

where R_0 is the electron Bohr radius, P_R is the average radiative rate, and ω_0 is the preexponential in the expression for the tunneling rate, taken here to be 10^{12} sec^{-1}. These expressions can be adapted to apply at high temperature by allowing for an additional nonradiative process corresponding to the ionization of the pair. For the sake of simplicity it is assumed that P_R and the nonradiative tunneling rate are independent of temperature, while the ionization rate P_I is temperature dependent. Equations (2) and (3) then become

$$Y_L = [P_R/(P_R + P_I)] \exp(-\tfrac{4}{3}\pi R_c^3 N_S) \ , \tag{4}$$

with

$$R_c = \tfrac{1}{2} R_0 \ln[\omega_0/(P_R + P_I)] \ . \tag{5}$$

In Fig. 6, Y_L is plotted versus N_S for various values of P_I corresponding to an increase of temperature. We assume average values of $P_R = 10^3$ sec^{-1} and $R_0 = 11$ Å as indicated by experiment.[7,9] In Fig. 6 it can be seen that as P_I increases the dependence of Y_L on N_S gets weaker. The reason is that the reduced lifetime of the pair due to the ionization process leaves less time available for tunneling to the defect. The temperature dependence of Y_L in different

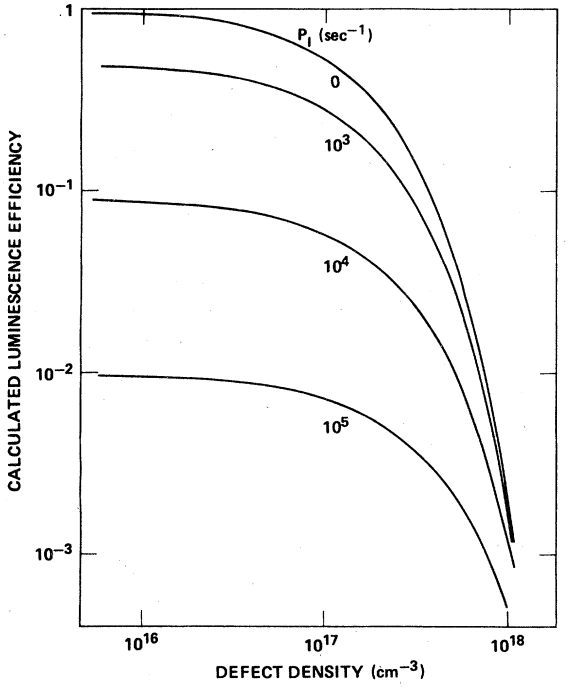

FIG. 6. Plot of the luminescence efficiency vs ESR spin density calculated from Eqs. (4) and (5). Values of $P_R = 10^3$ sec^{-1} and $R_0 = 11$ Å are assumed. The curves correspond to different values of P_I as indicated.

samples corresponds to vertical cuts in Fig. 6. Thus samples with a large N_S have a comparatively weak temperature dependence until a sufficiently high temperature is reached, above which Y_L is practically independent of N_S. This behavior is observed in Fig. 3 and therefore these results provide good confirmation of the tunneling model. Note that our analysis ignores such effects as a variation in band-tail width with different sample preparation conditions which would change P_I and alter the comparison of Y_L at high temperatures. Evidently such effects are of secondary importance in the samples measured.

C. Intensity dependence at high temperature

Figure 4 shows that at 170 K there is a region in which the quantum efficiency increases with excitation intensity G. The effect is most pronounced in samples of the lowest spin density, and is absent at 50 K when Y_L is independent of G. Our explanation is that at 170 K the majority of pairs are rapidly ionized. At low excitation intensity or at large defect densitites, the free carriers are sufficiently dilute that they always recombine nonradiatively by capture at localized gap states. However when the excitation rate is large enough or the defect density low enough, the probability of bimolecular, nongeminate, radiative

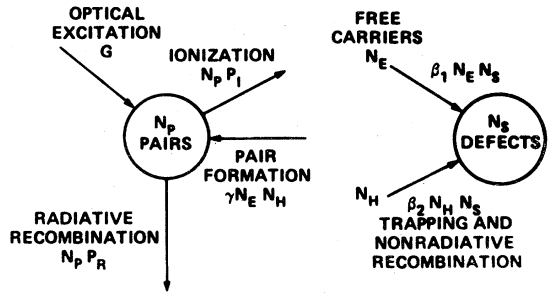

FIG. 7. Schematic recombination diagram showing N_P electron-hole pairs, N_E free electrons, N_H free holes, and N_S dangling-bond defeccts. The various generation, recombination, and trapping rates are shown.

recombination of the free carriers becomes significant, and provides in effect a second chance for luminescence. The situation is modeled in the rate diagram of Fig. 7. In steady-state N_P pairs, N_E free electrons and N_H free holes are assumed. The concept of a pair is not very precise, but is perhaps best defined as an electron and hole of separation less than about 50 Å. It is necessary to include pairs specifically in order to model the low-intensity geminate recombination. Pairs are generated directly by illumination with rate G, and by electron-hole collisions at rate $\gamma N_E N_H$. Pairs are lost by ionization and radiative recombination. In steady state the rate equation for the pairs is

$$\frac{dN_P}{dt} = 0 = G + \gamma N_E N_H - N_P P_I - N_P P_R \quad . \tag{6}$$

The luminescence efficiency is given by

$$Y_L(G) = N_P P_R / G = Y_0(1 + \gamma N_E N_H / G) \quad , \tag{7}$$

where $Y_0 = P_R/(P_R + P_I)$ which is the low intensity geminate limit. Clearly we must now introduce a nonradiative process to obtain a quantum efficiency other than unity. Figure 4 indicates the importance of dangling bonds with unpaired spins in the nonradiative process. However we ignore direct tunneling into the defect because of the discussion given in Sec. III B and because of the relatively low spin density in the samples measured. In support of his assumption we find at 170 K similar luminescence intensities at low G for all the samples investigated.

The most straightforward model assumes that free electrons and holes are captured by dangling bonds giving nonradiative recombination. (Note that we believe that this process is weakly radiative at a different energy.[17] This does not influence the present argument which is solely concerned with the band-edge transition.) From Fig. 7 the rate equation for free electrons is

$$\beta N_E N_S = N_P P_I - \gamma N_E N_H = G - N_P P_R \quad . \tag{8}$$

At 170 K, $N_P P_R/G\,(=Y_L) \ll 1$, and therefore

$$N_E \simeq G/\beta N_S \ . \tag{9}$$

If it is further assumed that the density of trapped carriers is small compared to N_E and N_H, then $N_H \simeq N_E$ and so

$$Y_L(G) = Y_0(1+\gamma G/\beta^2 N_S^2) \ . \tag{10}$$

This result gives a reasonably good description of the data. It predicts that at low G, Y_L is constant and given by the simple geminate model, while at high G, Y_L is enhanced by the bimolecular radiative process, by an amount inversely dependent on the spin density. These qualitative results are observed in the data of Fig. 4. The predicted dependence on G is only obeyed over at most two decades of G, and there are large departures at high G. This point is discussed further below. For each sample one can fit the intensity dependence of Y_L to the expression in Eq. (10) in the low intensity region. In Fig. 8, G_1, which is the value of G when $\gamma G/\beta^2 N_S^2 = 1$ obtained from these fits, is plotted versus the spin density, for all the samples measured. The dependence on N_S^{-2}

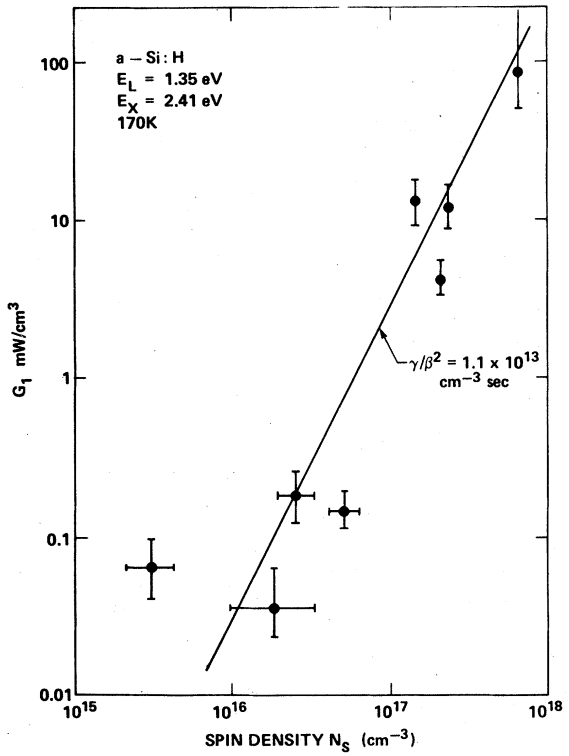

FIG. 8. A plot of G_1 vs spin density N_S for various undoped samples. G_1 is the value of G for which $\gamma G/\beta^2 N_S^2 = 1$, and is obtained by fitting intensity dependence data such as in Fig. 4 to Eq. (10). The solid line is the predicted behavior for a value of the parameter γ/β^2 of 1.1×10^{13} cm^{-3} sec.

predicted by Eq. (10) can now be clearly seen, despite some scatter in the data. Thus provided the excitation intensity is not too high, Eq. (10) is a good description of the recombination. We therefore conclude that the primary mechanism of nonradiative recombination above 100 K is the trapping of free carriers at singly occupied dangling-bond defects. This model is generally supported by photoconductivity measurements which find that in undoped samples, recombination is by electron trapping at states in the gap, although different states have previously been assumed.[18]

The scatter in the data points in Fig. 8 seems to be typical of the attempts to correlate luminescence and ESR measurements.[9] The origin of the scatter is not clear as there are various possible reasons. For example: (a) an inhomogeneous spin distribution in some samples, possibly including a surface spin density, and (b) the presence of defects without spins. These could be defects of the vacancy type, or possibly doubly occupied (or empty) dangling bonds due to inadvertent doping. A more significant discrepancy from Eq. (10) is the departure from the predicted dependence on G at high intensities. Again there are various possible explanations. For example the simple recombination model used to derive Eq. (10) may be inapplicable because: (a) No account is taken of the exponentially decreasing excitation rate in the bulk due to absorption of the incident light. The observed data therefore represent some average over the thickness of the illuminated region. Diffusion of the free carriers may also be significant. (b) At high excitation intensities the traps may saturate. (c) The distinction between free carriers and pairs becomes blurred at high G because the mean separation of particles decreases. Alternatively the turnover of Y_L at high G might indicate the onset of another nonradiative mechanism. Since this dominates at high intensity, an obvious candidate is an Auger process. As before, a reliable calculation of the expected rate is not available, but the effect apparently occurs when the photoexcited carrier density is sufficient to give reasonable overlap between carriers. Thus the Auger process seems a plausible explanation.

From the fit to Eq. (10) for the data shown in Fig. 8 we obtain,

$$\gamma/\beta^2 = 1.1 \times 10^{13}\ \text{cm}^{-3}\,\text{sec} \ , \tag{11}$$

with an uncertainty of about a factor 3. Mott *et al.*[19] have estimated the recombination rates under various circumstances and their discussion is followed here. The pair-formation process is an example in which ionization rather than recombination usually occurs, since we know that at 170 K, Y_L is small. γ is the rate of pair formation, and is related to the ionization probability P_I by

$$\gamma = R^3 P_I \exp(V/kT) \ , \tag{12}$$

where V is the Coulomb interaction of the electron-hole pair, and R is the radius of the pair. Assuming R is 50 Å,[9] a dielectric constant of 10, and taking an average value of P_l of 10^6 sec^{-1} from luminescence-decay data,[8] we obtain $\gamma \simeq 10^{-12}$ cm^3 sec^{-1}. This value of γ is not very sensitive to the exact value of R because the Coulomb term and the R^3 factor have opposite R dependences. From Eq. (11), $\beta \simeq 3 \times 10^{-13}$ cm^3 sec^{-1} is obtained. A comparable estimate of the trapping rate can in principle be obtained from photoconductivity data. However to the best of our knowledge this has not been evaluated. β can be predicted from a formula similar to Eq. (12), although in this case there should be no Coulomb interaction because the singly occupied dangling bond in neutral. Since the Coulomb term is relatively small, similar values of β and γ are expected. We therefore conclude that the trapping parameters obtained from the experiment are of reasonable magnitudes for the recombination model.

D. SUMMARY

Our main conclusions are as follows:

(1) The decrease of luminescence efficiency as the temperature is reduced below 50 K is a consequence of Auger recombination of neighboring pairs. The Auger process is observed at excitation densities exceeding about 10^{20} absorbed photons cm^{-3} sec^{-1}.

(2) The presence of singly occupied dangling bonds changes the temperature dependence of the luminescence through the mechanism in which an electron tunnels into the defect.

(3) The radiative and nonradiative processes at high temperature have been determined in greater detail. At low excitation intensities, luminescence is by geminate recombination. The rate-deteriming nonradiative path is ionization of the pairs, which is followed by nonradiative recombination of the free carriers at dangling bonds. At high excitation intensities, bimolecular radiative recombination can occur, particularly in samples of low spin density. The efficiency of this process depends on the capture rate of free carriers by dangling bonds.

(4) The recombination of free carriers is in reasonable quantitative agreement with a simple model of capture by singly occupied dangling bonds. As in previous measurements[9,17] we find no evidence for defects other than dangling bonds in the as-deposited material. The recombination process tends to be complicated by many effects, and it probably requires a combined study of luminescence, photoconductivity, and possibly drift mobility for a more detailed evaluation.

Finally, it should be pointed out that any attempt to interpret the temperature dependence of the luminescence must take into account the effects reported here. For example, the temperature dependence of the ionization rate can only be obtained if measurements are performed at low excitation intensities, and on samples with a spin density below about 10^{17}cm^{-3}.

ACKNOWLEDGMENTS

The author is grateful to J. C. Knights for providing samples. This work was supported by the Solar Energy Research Institute under Contract No. XJ-0-9079-1.

[1]D. Engemann and R. Fischer, in *Structure and Excitation of Amorphous Solids-1976,* edited by G. Lucovsky and F. L. Galeener, AIP Conf. Proc. No. 31 (AIP, New York, 1976), p. 37.
[2]J. I. Pankove and D. E. Carlson, Appl. Phys. Lett. 29, 620 (1976).
[3]R. A. Street, Philos. Mag. B 37, 35 (1978).
[4]I. G. Austin, T. S. Nashashibi, T. M. Searle, P. G. LeComber, and W. E. Spear, J. Non-Cryst. Solids 32, 373 (1979).
[5]S. Kurita, W. Czaja, and S. Kinmond, Solid State Commun. 32, 879 (1979).
[6]M. A. Paesler and W. Paul, Philos. Mag. B 41, 393 (1980).
[7]C. Tsang and R. A. Street, Phys. Rev. B 19, 3027 (1979).
[8]J. Noolandi, K. M. Hong, and R. A. Street, Solid State Commun. 34, 45 (1980).
[9]R. A. Street, J. C. Knights, and D. K. Biegelsen, Phys. Rev. B 18, 1880 (1978).
[10]R. W. Collins, M. A. Paesler, G. Moddel, and W. Paul, J. Non-Cryst. Solids 35–36, 681 (1980).
[11]R. A. Street and D. K. Biegelsen, Solid State Commun. 33, 1159 (1980).
[12]C. Tsang and R. A. Street, Philos. Mag. 37, 601 (1978).
[13]W. Rehm and R. Fischer, Phys. Status Solidi B 94, 595 (1979).
[14]D. F. Nelson, J. D. Cuthbert, P. J. Dean, and D. G. Thomas, Phys. Rev. Lett. 17, 1262 (1966).
[15]See, for example, P. T. Landsberg and D. J. Robbins, Solid State Electronics 21, 1289 (1978), and references therein.
[16]W. Schmidt, Phys. Status Solidi 84, 529 (1977).
[17]R. A. Street, Phys. Rev. B 21, 5775 (1980).
[18]D. A. Anderson and W. E. Spear, Philos. Mag. 36, 695 (1977).
[19]N. F. Mott, E. A. Davis, and R. A. Street, Philos. Mag. 32, 961 (1975).